



1 **Three distinct Holocene intervals revealed in NW Madagascar:**  
2 **evidence from two stalagmites from two caves, and implications for**  
3 **ITCZ dynamics**

4

5 Voarintsoa, Ny Riavo G.<sup>1\*</sup>, L. Bruce Railsback<sup>1</sup>, George A. Brook<sup>2</sup>, Lixin Wang<sup>2</sup>, Gayatri Kathayat<sup>3</sup>,  
6 Hai Cheng<sup>3,4</sup>, Xianglei Li<sup>3</sup>, R. Lawrence Edwards<sup>4</sup>, Rakotondrazafy Amos Fety Michel<sup>5</sup>, Madison  
7 Razanatseheno Marie Olga<sup>5</sup>

8

9 <sup>1</sup> Department of Geology, University of Georgia, Athens, GA 30602-2501 U.S.A.

10 <sup>2</sup> Department of Geography, University of Georgia, Athens, Georgia, 30602-2502 U.S.A.

11 <sup>3</sup> Institute of Global Environmental Change, Xi'an Jiaotong University, Xi'an, Shaanxi 710049, P.R. China

12 <sup>4</sup> Department of Earth Sciences, University of Minnesota, Minneapolis, Minnesota 55455, U.S.A.

13 <sup>5</sup> Department of Geology, University of Antananarivo, Madagascar

14

15 \*Correspondence to: Ny Riavo Voarintsoa ([nv1@uga.edu](mailto:nv1@uga.edu) or [nyriavony@gmail.com](mailto:nyriavony@gmail.com))

16 **ABSTRACT**

17 Petrographic features, mineralogy, and stable isotopes from two stalagmites collected  
18 from Anjohibe and Anjokipoty Cave allow distinction of three intervals of the Holocene in  
19 northwestern Madagascar. The Malagasy early Holocene interval (between ca. 9.8 and 7.8 ka) was  
20 wet, and vegetation changes seem to have been controlled by changes in climate. The Malagasy  
21 late Holocene interval (after ca. 1.6 ka) also records evidence of wet conditions, but changes in  
22 vegetation were influenced by anthropogenic effects, as suggested by the stalagmite  $\delta^{13}\text{C}$  shift.  
23 The Malagasy middle Holocene interval seems to be characterized by drier conditions, relative to  
24 the early and late Holocene.

25 The alternating wet/dry/wet conditions in northwestern Madagascar during each of these  
26 Holocene intervals could be linked to the long-term migration of the Inter-Tropical Convergence  
27 Zone (ITCZ). Higher southern hemisphere (SH) insolation and globally colder conditions drove the  
28 ITCZ's mean position further south, bringing more rainfall to northwestern Madagascar. This  
29 condition was favorable for stalagmite deposition. In contrast, higher northern hemisphere (NH)  
30 insolation and globally warmer conditions displaced the ITCZ further north, bringing less rainfall to  
31 northwestern Madagascar. This condition was not favorable for stalagmite deposition.

32 The linkage between global cooling and wet conditions in regions of the SH, in response to  
33 the southward migration of the ITCZ, is further exemplified at centennial scale by the negative



34  $\delta^{18}\text{O}$  and  $\delta^{13}\text{C}$  values in northwestern Madagascar during the 8.2 ka cold event when the Atlantic  
35 Meridional Overturning Circulation (AMOC) weakened. Weakening of the AMOC led to an  
36 enhanced temperature gradient between the two hemispheres, i.e. cold NH and warm SH, shifting  
37 the mean position of the ITCZ further south. This brought wet conditions in the SH monsoon  
38 regions, such as northwestern Madagascar, and dry conditions in the NH monsoon regions,  
39 including the Asian Monsoon and the East Asian Summer Monsoon. This climatic relationship is  
40 useful to test for climate models that are used to predict changes in future climate.

41

## 42 1. Introduction

43 Although much is known about the Holocene climate change worldwide (Mayewski et al.,  
44 2004; Wanner and Ritz, 2011; Wanner et al., 2011; 2015), high-resolution climate data for the  
45 Holocene period is still regionally limited in the Southern Hemisphere (e.g. Wanner et al. 2008;  
46 Marcott et al. 2013; Wanner et al., 2015). This uneven distribution of data hinders our  
47 understanding of the spatio-temporal characteristics of Holocene climate change, including our  
48 understanding of the most important climate forcings of the Holocene. Some of these forcings  
49 would, for example, have an influence on the ITCZ behavior and the monsoonal response in low-  
50 to mid-latitude regions (e.g. Wanner et al., 2015; Talento and Barreiro, 2016). Madagascar is  
51 particularly a strategic location where such records are needed because it holds a key position in  
52 the Indian Ocean (Fig. 1a), and it is seasonally visited by the ITCZ (Inter-Tropical Convergence Zone)  
53 with a karst region crossing latitudinal belts (Fig. 1c). Thus, records from Madagascar could  
54 complete gaps in paleoclimate reconstruction in the Southern Hemisphere (SH). Records from  
55 Madagascar could also help refine paleoclimate simulations that could provide better  
56 understanding of the global circulation and the land-atmosphere-ocean interaction during the  
57 Holocene.

58 To fill the knowledge gap about the Holocene climate change in the SH and particularly in  
59 Madagascar, and to better understand the paleohydrology in NW Madagascar during the  
60 Holocene, we present multiproxy records (stable isotopes, petrography, mineralogy, variability of  
61 layer-specific width) from stalagmites from two caves, Anjohibe and Anjokipoty Caves, in  
62 northwestern Madagascar. Stalagmites are used because of their potential in storing significant



63 climatic information (e.g. Fairchild and Baker, 2012, p. 9–10), and in Anjohibe cave, recent studies  
64 have shown the replicability of paleoclimate records from stalagmites (e.g. Burns et al., 2016). The  
65 two stalagmites investigated here provide replication of paleoclimate records, which allow us to  
66 characterize the Holocene climate change in northwestern Madagascar. First we infer the climatic  
67 significance from direct interpretation of the stalagmite records. With a better understanding of  
68 Madagascar's paleoclimate, we will then investigate on the possible climatic drivers of tropical  
69 climate changes to draw a more comprehensive conclusion on the major factors controlling its  
70 hydrological cycle.

## 71 2. Setting

### 72 2.1. Regional environmental setting

73 Two stalagmites, ANJB-2 and MAJ-5, were collected from Anjohibe and Anjokipoty caves,  
74 respectively, in the region of Majunga of northwestern Madagascar (Fig. 1). Anjohibe (S15° 32'  
75 33.3"; E046° 53' 07.4") and Anjokipoty (S15° 34' 42.2"; E046° 44' 03.7") are separated by about  
76 16.5 km (Fig. 1c). Their location in the zone visited by the ITCZ (e.g. Nassor and Jury, 1998) makes  
77 them a good place to test for the latitudinal migration of the ITCZ (e.g. Chiang and Bitz, 2005;  
78 Broccoli et al., 2006; Chiang and Friedman, 2012; Schneider et al., 2014). The ITCZ brings north or  
79 northwesterly monsoon winds to Madagascar during austral summers, in a pattern that the  
80 Service Météorologique of Madagascar calls the "Malagasy monsoon". Majunga's climate in  
81 general belongs to the tropical savanna climate (Aw) of Köppen-Geiger climate classification, with  
82 distinct wet summer (from October to April) and dry winter (May-September). The mean annual  
83 rainfall is around 1160 mm. The mean maximum temperature in November, the hottest month in  
84 the summer, is about 32°C. The mean minimum temperature in July, the coldest month of the dry  
85 winter, is about 18°C (Fig. 1b).

86 Anjohibe and Anjokipoty caves have provided many insights about the paleoenvironmental  
87 and archaeological history of northwestern Madagascar (e.g. Burney et al., 1997, 2004; Brook et  
88 al., 1999; Gommerly et al., 2011; Jungers et al., 2008; Vasey et al., 2013; Burns et al., 2016).  
89 Replicability of stable isotope records from Anjohibe Cave stalagmites (e.g. Burns et al., 2016)  
90 further suggests the potential of stalagmites to provide robust paleoclimate information for  
91 Madagascar.



92

## 93 **2.2. The Holocene in northwestern Madagascar**

94 Little is known about Holocene climate change in northwestern Madagascar, and little is  
95 also known about the major drivers of long-term climatic changes there. Most paleoclimate  
96 information from northwestern Madagascar covers the last two millennia with more focus on the  
97 anthropogenic effects on the Malagasy ecosystems (e.g. Crowley and Samonds, 2013; Burns et al.,  
98 2016). This is because several studies revealed coincidence of Madagascar's megafaunal extinction  
99 with human arrival around 2-3 ka BP (e.g. see Table 1 of Virah-Sawmy et al., 2010; MacPhee and  
100 Burney, 1991; Burney et al., 1997c; Crowley, 2010). Long-term records are very scarce. The only  
101 records that cover longer time interval were sediment cores collected from Lake Mitsinjo (3,500  
102 yr. BP; Matsumoto and Burney, 1994) and cave sediments from Anjohibe Cave (40,000 yr. BP;  
103 Burney et al. 1997). Both sediments provided useful information about the paleoenvironmental  
104 changes in northwestern Madagascar, but linkages to global climatic changes were not fully  
105 understood. Madagascar is however a key location in the SH that could provide meaningful  
106 paleoclimate information about the global circulation during the Holocene.

## 107 **3. Methods**

108 Stalagmites ANJB-2 and MAJ-5 were radiometrically dated using the multi-collector ICP-  
109 MS of the University of Minnesota, USA and of the Stable Isotopes Laboratory of Xi'an, in Jiaotong,  
110 China. Twenty-two powdered samples of approximately 50 to 200 mg were extracted from  
111 Stalagmite ANJB-2 and nine samples from Stalagmite MAJ-5 (Tables S1 and S2). The stalagmites'  
112 chronology was constructed using the StalAge1.0 algorithm of Scholz and Hoffman (2011) and  
113 Scholz et al. (2012). The StalAge scripts were run on the statistics program R version 3.2.2 (2015-  
114 08-14). The age models were adjusted in respect to identified hiatal surfaces, implementing the  
115 approach of Railsback et al. (2013; see their Fig. 9).

116 Petrography and mineralogy of the two stalagmites were investigated using hand samples'  
117 polished surfaces and a scanned image of it (measuring the layer-specific width), microscopic  
118 observation of eleven oversized thin sections (3 x2 in), and X-ray diffraction of powdered spelean  
119 layers with CoK $\alpha$  radiation at a 2 $\theta$  angle between 20° and 60° using a Bruker D8 X-ray  
120 Diffractometer of the Department of Geology of the University of Georgia.



121 Oxygen and carbon isotope ratios were measured using the Finnigan MAT-253 mass  
122 spectrometer fitted with the Kiel IV Carbonate Device of the Xi'an Stable Isotope Laboratory in  
123 China (ANJB-2; n=654) and using the Delta V Plus at 50°C fitted with the GasBench-IRMS machine  
124 of the Alabama Stable Isotope Laboratory in USA (MAJ-5; n=286). Analytical procedures using the  
125 MAT 253 are identical to those described in Dykoski et al. (2005), with isotopic measurement  
126 errors of less than 0.1 ‰ for both  $\delta^{13}\text{C}$  and  $\delta^{18}\text{O}$ . Analytical methods and procedures using the  
127 GasBench-IRMS machine are identical to those described in Skrzypek and Paul (2006), Paul and  
128 Skrzypek (2007), and Lambert and Aharon (2011), with  $\pm 0.1$  ‰ errors for both  $\delta^{13}\text{C}$  and  $\delta^{18}\text{O}$ . In  
129 both techniques, the results were reported relative to Vienna PeeDee Belemnite (VPDB) and with  
130 standardization relative to NBS19. Inter-lab comparison of the isotopic results was done by  
131 replicating every tenth sample of Stalagmite MAJ-5 on the MAT 253 mass spectrometer. The  
132 replicates suggest strong correlation (Fig. S4). Finally, the  $\delta^{18}\text{O}$  and  $\delta^{13}\text{C}$  of the spelean aragonite  
133 were transformed, by a subtraction of 1.7 ‰ (Romanek et al., 1992) and 0.8‰ (Kim et al., 2007)  
134 respectively. These transformations were done here to compensate for the aragonite's inherent  
135 fractionation of heavier isotopes as have been done in previous studies (e.g. Sletten et al., 2013;  
136 Voarintsoa et al., 2016, in revision). With these transformations, the corrected isotopic values  
137 remove the mineralogical bias in isotopic interpretation between calcite and aragonite.

## 138 4. Results

### 139 4.1. Radiometric data

140 Results from radiometric analyses of the two stalagmites are presented in Table S1 and  
141 Table S2. Stalagmite ANJB-2 has a  $^{234}\text{U}$  range from  $64 \pm 0$  to  $9833 \pm 44$  ppb and a  $^{232}\text{Th}$  range from  
142  $180 \pm 8$  to  $39850 \pm 809$  ppt. Corrected  $^{230}\text{Th}$  suggests that it was deposited between ca.  $8977 \pm 50$   
143 and  $161 \pm 64$  yr. BP. Stalagmite MAJ-5 has a  $^{234}\text{U}$  range from  $1224 \pm 4$  to  $12609 \pm 83$  ppb and a  $^{232}\text{Th}$   
144 range from  $3044 \pm 63$  to  $38990 \pm 842$  ppt. Corrected  $^{230}\text{Th}$  suggests that it was deposited between  
145 ca.  $9796 \pm 64$  and  $150 \pm 24$  yr. BP. Those age ranges most completely span the Holocene interval in  
146 northwestern Madagascar. StalAge model and petrography highlight three distinct intervals of the  
147 Holocene (Fig. 2): (1) between ca. 9.8 and 7.8 ka BP, with evidence of  $\text{CaCO}_3$  deposition, (2)  
148 between ca. 7.8 and 1.6 ka BP, with a noticeable long-term hiatus, and (3) after ca. 1.6 ka BP when  
149 the stalagmites resumed to grow. These intervals will be called Malagasy early Holocene interval



150 (MEHI), Malagasy mid-Holocene interval (MMHI), and Malagasy late Holocene interval (MLHI)  
151 respectively.

152

#### 153 4.2. Stable isotopes

154 Raw values of  $\delta^{18}\text{O}$  and  $\delta^{13}\text{C}$  for Stalagmite ANJB-2 range from  $-8.85$  to  $-2.27\text{‰}$ , and from  
155  $-11.00$  to  $+5.15\text{‰}$ , respectively, relative to VPDB. The mean values are  $-4.97\text{‰}$  and  $-4.18\text{‰}$   
156 respectively for  $\delta^{18}\text{O}$  and  $\delta^{13}\text{C}$ . Raw values of  $\delta^{18}\text{O}$  and  $\delta^{13}\text{C}$  in Stalagmite MAJ-5 range from  $-8.80$   
157 to  $-0.85\text{‰}$ , and from  $-9.44$  to  $+2.60\text{‰}$ , respectively, relative to VPDB. The mean values are  $-$   
158  $4.85\text{‰}$  and  $-4.38\text{‰}$  respectively for  $\delta^{18}\text{O}$  and  $\delta^{13}\text{C}$ , but distinguishable between MEHI and the  
159 MLHI (Fig. 3). In both stalagmites, the amplitude of  $\delta^{18}\text{O}$  fluctuations stayed constant throughout  
160 the Holocene; whereas the  $\delta^{13}\text{C}$  profile shows a dramatic shift toward greater values (i.e. from  $-$   
161  $10.90\text{‰}$  to  $+3.75\text{‰}$ , VPDB) at ca. 1.5 ka BP. Values of  $\delta^{13}\text{C}$  only parallel those of  $\delta^{18}\text{O}$  during the  
162 MEHI (Fig. 3).

163 The MEHI and the MLHI are isotopically distinct (Fig. 3a). The MEHI is characterized by  
164 statistically correlated  $\delta^{18}\text{O}$  and  $\delta^{13}\text{C}$  ( $r^2=0.65$  and  $0.53$ ), and much depleted  $\delta^{13}\text{C}$  values (ca.  $-11.0$   
165 to  $-4.0\text{‰}$ ). The 8.2 ka event, a widespread event in the NH (e.g. Alley et al., 1997), is also identified  
166 in the stalagmite records. Stalagmite  $\delta^{18}\text{O}$  and  $\delta^{13}\text{C}$  values both decreased to a minimum of  $-6.78$   
167 and  $-10.88\text{‰}$ , respectively at that interval (Figs. 3 and 7). In contrast to the MEHI, the MLHI's  $\delta^{18}\text{O}$   
168 and  $\delta^{13}\text{C}$  are poorly correlated ( $r^2=0.25$  and  $0.17$ ), and  $\delta^{13}\text{C}$  values are more enriched (Fig. 3).

169

#### 170 4.3. Mineralogy, petrography, and layer-specific width

171 In both stalagmites, the hiatus of deposition (see Sect. 4.1) is characterized by a well-  
172 developed Type L surface (Figs. 2b, 6S). Petrography and mineralogy are distinct before and after  
173 that hiatus (Fig. 2). Below the hiatus, laminations are well preserved in both stalagmites. Above  
174 the hiatus, laminations are not well-preserved, although noted at some intervals.

175 In Stalagmite ANJB-2, the layer-specific width varies from 37 to 26.5 mm with a mean of  
176 30 mm. It narrows to 28 mm at the hiatus (Fig. 2b). Below the hiatus, mineralogy is dominated by  
177 aragonite, although a few thick layers of calcite are also identified. A thin ( $\sim 2\text{-}3$  mm) but  
178 remarkable layer of white, very soft, and porous aragonite is identified just below the hiatus (Fig.



179 S6). This layer is capped with a very thin layer of dirty material. Above the hiatus, mineralogy is  
180 also composed of calcite and aragonite, with dominance of calcite, and the calcite layers contain  
181 some macro-cavities that are mostly off-axis macroholes (Shtober-Zisu et al., 2012).

182 In Stalagmite MAJ-5, the layer specific width varies from 50 to 22 mm with a mean of 35.5  
183 mm. It narrows to 22 mm at the hiatus (Fig. 2b). Below the hiatus, mineralogy is a mixture of calcite  
184 and aragonite. Above the hiatus, mineralogy is mainly calcite and macro-cavities are also  
185 distributed throughout that upper part of the stalagmite.

186

#### 187 4.4. Summary of the results

188 The records from Stalagmites ANJB-2 and MAJ-5 suggest three distinct intervals of the  
189 Holocene. The MEHI (between ca. 9.8 and 7.8 ka BP), with evidence of stalagmite deposition, is  
190 characterized by statistically correlated  $\delta^{18}\text{O}$  and  $\delta^{13}\text{C}$  ( $r^2=0.65$  and  $0.53$ ) and more negative  $\delta^{13}\text{C}$   
191 values (ca.  $-11.0$  to  $-4.0$  ‰). The MMHI (between ca. 7.8 to 1.6 ka BP) is marked by a long-term  
192 hiatus of deposition, which is preceded by a well-developed Type L surface in both Stalagmite  
193 ANJB-2 and MAJ-5 (Fig. 2; Fig. S6). The Type L surface is observed as an upward narrowing of the  
194 stalagmite's width and layer thickness. It is particularly well-developed in Stalagmite MAJ-5 (Fig.  
195 S6). In the other Stalagmite ANJB-2, the hiatus at the Type L surface is preceded by approximately  
196 3 mm-thick layer of highly porous, very soft, and fibrous white crystals of aragonite (the only  
197 aragonite with such properties), and it is topped by a thin and well-defined layer of detrital  
198 materials (Fig. S6), further supporting the presence of a hiatus. Finally, the MLHI (after ca. 1.6 ka  
199 BP) is characterized by poorly correlated  $\delta^{18}\text{O}$  and  $\delta^{13}\text{C}$  ( $r^2=0.25-0.17$ ). This interval is additionally  
200 marked by a shift in  $\delta^{13}\text{C}$  and greater  $\delta^{13}\text{C}$  (Fig. 3).

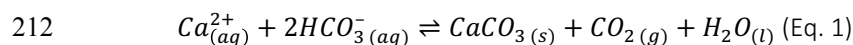
201



## 202 5. Discussion

### 203 5.1. Paleoclimate significance of stalagmite growth and non-growth: implications for 204 paleohydrology

205 Stalagmites are secondary cave deposits, which are CaCO<sub>3</sub> precipitates from cave  
206 dripwater. Calcium carbonate precipitation occurs by CO<sub>2</sub> degassing, which increases the pH of the  
207 dripwater and thus increases the concentration of CO<sub>3</sub><sup>2-</sup>. In some cases, evaporation, which  
208 increases the Ca<sup>2+</sup> and/or CO<sub>3</sub><sup>2-</sup> of the dripwater, may also be important. Degassing occurs because  
209 the high-PCO<sub>2</sub> water from the epikarst meets the low-PCO<sub>2</sub> cave air, while evaporation occurs  
210 when humidity inside the cave is relatively low. The fundamental equation for stalagmite  
211 deposition is shown in Eq. 1.



213 Growth and non-growth of stalagmites depends on several factors that could be mainly  
214 linked to water availability, which in turn is linked to climate (more water during warm/rainy  
215 seasons and less water during cold/dry seasons). Water is the main dissolution and transport agent  
216 for most chemicals in speleothems. Cave hydrology varies significantly over time in response to  
217 climate, and this variability influences the formation or dissolution of CaCO<sub>3</sub>. In this regard, calcium  
218 carbonate does not form if the water feeding the cave is very little to absent, or if it is too much.  
219 Absence of groundwater recharge most typically occurs during extremely dry conditions, whereas  
220 excessive water input to the cave occurs during extremely wet conditions. In the latter scenario,  
221 water is undersaturated and flow rates are too fast to allow degassing. Oftentimes, water  
222 availability could be reflected in the extent of vegetation above and around the cave, as this  
223 requires enough moisture from the soil or from the shallow groundwater. Surface biomass  
224 supplies most of the CO<sub>2</sub> to the soil epikarst, and this could contribute to the stalagmites'  
225 processes of formation. Growth and non-growth of stalagmites could be associated with cave  
226 dripwater fed by atmospheric precipitation, and this could be linked to climatic conditions at the  
227 time when stalagmites grew.

228 Major hiatuses in stalagmite deposition could be marked by variety of features, including  
229 the presence of erosional surfaces, chalkification, dirt bands/detrital layers, deviation of growth  
230 axis, and/or sometimes by color changes (e.g. Holmgren et al., 1995; Dutton et al., 2009; Railsback





231 et al., 2013; Railsback et al., 2015; Voarintsoa et al., 2016; this study). Railsback et al. (2013) were  
232 specifically able to identify significant features in stalagmites that allow distinction between non-  
233 deposition during extremely wet (Type E) and non-deposition during extremely dry conditions  
234 (Type L; Fig. 2b). Physical properties of stalagmites that support these extreme dry and wet events  
235 are summarized in Table 1 of Railsback et al. (2013) and the mechanism is explained in their figure  
236 5.

237 Type E surfaces are layer-bounding surfaces between two spelean layers when the  
238 underlying layers show evidence of truncation. The truncation results from dissolution or erosion  
239 (thus the name “E”) of the previously-formed layers of stalagmites by abundant undersaturated  
240 water. Type E surfaces are commonly capped with a layer of calcite (Railsback et al., 2013). This  
241 mineralogical trend is not surprising in stalagmites as calcite commonly forms under wetter  
242 conditions (e.g. Murray, 1954; Pobeguín, 1965; Siegel, 1965; Thrailkill, 1971; Cabrol and Coudray,  
243 1982; Railsback et al. 1994; Frisia et al., 2002). Additionally, non-carbonate detrital materials are  
244 commonly abundant with varying grain size (i.e. from silt- to sand-size; Railsback et al., 2013).

245 Type L surfaces, on the other hand, are layer-bounding surfaces where the layers became  
246 narrower upward and thinner toward the flank of the stalagmite. The decrease in thickness and  
247 width of the stalagmites upward is an indication of lessening in deposition (thus the name “L”;  
248 Railsback et al., 2013). Aragonite is a very common mineralogy below the surface, especially in  
249 warmer settings. Layers of aragonite commonly form under drier conditions (Murray, 1954;  
250 Pobeguín, 1965; Siegel, 1965; Thrailkill, 1971; Cabrol and Coudray, 1982; Railsback et al. 1994;  
251 Frisia et al., 2002). Non-carbonate detrital materials are scarce, and if they are present, they tend  
252 to form a very thin horizon of very fine dust material (Railsback et al., 2013), typical characteristics  
253 for a hiatus in deposition. Identification of Type L surfaces has been aided by measuring the layer-  
254 specific width, or LSW (e.g. Sletten et al., 2013; Railsback et al., 2014), an approach that is also  
255 performed in this study.

256

## 257 5.2. Holocene climate reconstruction in northwestern Madagascar

258 Although the specific boundaries between the early, mid, and late Holocene have been  
259 proposed for global application (Walker et al., 2012; Head and Gibbard, 2015), their use is still



260 spatially limited (e.g. Wanner et al., 2015). The age models and the petrographic features of  
261 Stalagmites ANJB-2 and MAJ-5 suggest three distinct but different intervals (MEHI, MMHI, and  
262 MLHI) that could be used to characterize the Holocene in northwestern Madagascar, as proposed  
263 in Section 4.1. These intervals are modeled in the three simplified sketches of Figure 4. In this  
264 paper, these Malagasy intervals were provided here not to argue against the previously proposed  
265 intervals of the Holocene (Walker et al., 2012; Head and Gibbard, 2015). Instead, they were  
266 adopted here to ease discussion of the available records. For comparison, those intervals are  
267 shown in Fig. 4d.

268

#### 269 5.2.1. Malagasy early Holocene interval (between ca. 9.8 to ca. 7.8 ka BP)

270 Stalagmite deposition during the early Holocene suggests that Anjohibe and Anjokipoty  
271 caves were sufficiently supplied with water to allow  $\text{CaCO}_3$  precipitation, in accord with Eq.1. This  
272 in turn implies relatively wet conditions that could reflect longer summer rainy seasons, or wet  
273 years in northwestern Madagascar (see Supplementary Text 1 and Fig. S9). The correlative  $\delta^{13}\text{C}$   
274 and  $\delta^{18}\text{O}$  values further suggest that vegetation consistently responded to changes in moisture  
275 availability, which in turn is dependent on climate.

276 One striking aspect we found in Stalagmite ANJB-2 is the local minima in  $\delta^{18}\text{O}$  ( $\sim -6.78\text{‰}$ )  
277 and  $\delta^{13}\text{C}$  ( $\sim -11.00\text{‰}$ ) centered at 8.2 ka BP (Figs 3 and 7). X-ray diffraction data for this period, at  
278 195–202 mm from the top of the stalagmite, suggest that the mineralogy at that age is calcite (Fig.  
279 S8). The decrease in stable isotopes of oxygen and carbon and the presence of calcite mineralogy  
280 at the same interval combine to suggest a wet 8.2 ka event in northwestern Madagascar. The 8.2  
281 ka event is a prominent cold event in the northern Atlantic records and many NH terrestrial  
282 records. It may have been triggered by a release of freshwater from the melting Laurentide ice  
283 sheet into the North Atlantic basin (e.g. Alley et al., 1997; Barber et al., 1999). Freshwater influx  
284 to the Atlantic could have altered the Atlantic Meridional Overturning Circulation, and could  
285 eventually influence the climate of Madagascar (Sect. 5.3.3). The  $\delta^{18}\text{O}$  and  $\delta^{13}\text{C}$  records from  
286 Stalagmite ANJB-2 show similar features as the  $\delta^{18}\text{O}$  of the Greenland ice core records (GRIP and  
287 NGRIP, Fig. 7), and suggest that the cold 8.2 ka event in the Northern Hemisphere records coincide  
288 with wet period in northwestern Madagascar. This is the first time in our records that reveals a



289 strong link between paleoenvironmental changes in Madagascar and abrupt climatic events in the  
290 Northern Hemisphere records, suggesting that Madagascar climate was also very sensitive to such  
291 abrupt climate events.

292

### 293 **5.2.2. Malagasy mid-Holocene interval (ca. 7.8 to 1.6 ka BP)**

294 The mid-Holocene hiatus in both stalagmites could be interpreted in two ways: an interval  
295 of extremely wet conditions or an interval of extremely dry conditions. In the scenario of extremely  
296 wet conditions, the dripwater rate must have been very high to allow degassing, thus inhibiting  
297  $\text{CaCO}_3$  precipitation. The excesses of water infiltrating into the cave could have dissolved  
298 previously deposited stalagmite layers. However, the absence of a major Type E surface (erosional  
299 surface; Railsback et al., 2013) at the hiatus suggests that extreme wet conditions did not prevail  
300 during the mid-Holocene.

301 In the case of extremely dry conditions, the cave must have not received sufficient  
302 dripwater to allow the stalagmites to grow. Several lines of evidence in both stalagmites suggest  
303 a dry mid-Holocene in northwestern Madagascar. First, the major Type L surfaces identified in  
304 Stalagmite MAJ-5 and ANJB-2 at ca. 62 and 117 mm respectively from the top of each stalagmite  
305 suggest that the mid-Holocene was drier. In Stalagmite ANJB-2, this Type L surface is preceded by  
306 a thin (ca. 3 mm) layer of aragonite, a  $\text{CaCO}_3$  polymorph frequently found in stalagmites to indicate  
307 intervals of drier conditions (Murray, 1954; Pobeguín, 1965; Siegel, 1965; Thrailkill, 1971; Cabrol  
308 and Coudray, 1982; Railsback et al. 1994; Frisia et al., 2002). This Type L is also capped with a very  
309 thin layer of dust materials, similar to the layer described in Railsback et al. (2013). This inference  
310 of drier mid-Holocene interval is additionally supported by a decrease in the layer-specific width  
311 of the stalagmites towards the hiatus (Fig. 2B), quantifying the decrease in  $\text{CaCO}_3$  deposition,  
312 which could have started at the end of the early Holocene and continued to the mid-Holocene.

313 Although records are missing during the mid-Holocene in both of our stalagmites, the  
314 absence of stalagmite deposition at a major Type L surface (Fig. 2), which is preceded by a thin  
315 porous layer of aragonite, would very likely suggest that the cave was not sufficiently supplied with  
316 water, and thus climate was drier than compared to the early Holocene, hence we name it  
317 “Malagasy mid-Holocene dry period”. The dry mid-Holocene was also felt in other regions of



318 Madagascar (e.g. Gasse and Van Campo, 1998; Virah-Sawmy et al., 2009). Drier intervals in  
319 northwestern Madagascar would imply drier summer seasons with less rainfall (reflecting a short  
320 visit of the ITCZ), rather than simply dry climate with no rainfall at all (see Supplementary Text 1  
321 and Fig. S9). It is therefore possible to expect that at some locations in the cave, some stalagmites  
322 could still grow but very slowly, such as ANJ94-5 (Wang and Brook, 2013, Wang, 2016).

323

### 324 **5.2.3. Malagasy late Holocene interval (ca. 1.6 ka to present)**

325 The resumption of stalagmite deposition after ca. 1.6 ka BP suggests that climate in  
326 northwestern Madagascar returned to relatively wet conditions, at least similar to the early  
327 Holocene climate conditions. Stable isotopes of carbon ( $\delta^{13}\text{C}$ ) profile display a shift from depleted  
328 to enriched values at ca. 1.5 ka BP (Fig. 3; Fig. S7), as have been observed in previous stable isotope  
329 profiles in Anjohibe (e.g. Burns et al., 2016; Voarintsoa et al., in revision), suggesting that the late  
330 Holocene's vegetation was different from that of the early Holocene. This shift has been linked to  
331 a change from a  $\text{C}_3$ -dominated landscape to a  $\text{C}_4$ -dominated landscape, the cause of which has  
332 been linked to recent human activities (e.g. Crowley and Samonds, 2013; Burns et al., 2016;  
333 Crowther et al., 2016). The decrease in  $\delta^{13}\text{C}$  in Stalagmite MAJ-5 after 0.8 ka BP (Fig. 3), compared  
334 to the high  $\delta^{13}\text{C}$  of Stalagmite ANJB-2, is open to further investigation as to whether linked to local  
335 vegetation highly disturbed by human activities, cave micro-climate, or some other problems  
336 encountered during chemical analyses.

337 Although the last ca. 1.6 ka BP interval records overall wetter conditions, it was also  
338 interrupted by some occasional dryness, as suggested by several positive peaks in the Stalagmite  
339  $\delta^{18}\text{O}$  records. Drier intervals during the late Holocene were, for example, revealed in Anjohibe  
340 between ca. AD 755 and 795 (i.e. 1195–1155 yr. BP; Voarintsoa et al.'s, in revision), and in previous  
341 paleoenvironmental studies, in which a peak drought around 1300–950 Cal BP was reported  
342 (Burney, 1987a, b; Burney, 1993; Matsumoto and Burney, 1994; Virah-Sawmy et al., 2009).

343

### 344 **5.3. Holocene climate in northwestern Madagascar: implications for the ITCZ dynamics**

345 The periods of deposition of the two stalagmites ANJB-2 and MAJ-5 from Anjohibe and  
346 Anjokipoty Caves respectively during the MEHI and the MLHI suggests that these intervals were



347 relatively wetter than the MMHI. The absence of an increasing trend in the  $\delta^{18}\text{O}$  values, with a  
348 consistent amplitude of fluctuations, throughout the Holocene suggest that northwestern  
349 Madagascar has been consistently visited by the ITCZ. However, the alternating wet/dry/wet  
350 intervals during the early, mid, and late Holocene suggest that, in addition to the seasonal  
351 migration of the ITCZ, these long-term climate changes could be associated with the duration of  
352 the ITCZ visit in the Southern Hemisphere, leading to wet or dry years in Madagascar (also see  
353 Supplementary Text 1 and Fig. S9).

354 The length of visit of the ITCZ in northern or southern hemisphere has been linked to the  
355 latitudinal shift or latitudinal migration of the ITCZ. When the ITCZ's mean position is south (often  
356 mentioned in several papers as southward migration of the ITCZ), many regions in the southern  
357 Hemisphere become wetter because summer rainy seasons get longer (e.g. Voarintsoa et al.,  
358 2016), and monsoonal rainfall during summer seasons could have intensified. When the ITCZ's  
359 mean position is north (i.e. referred usually as a northward migration of the ITCZ), many regions  
360 in the southern hemisphere become drier as summer rainy seasons become shorter, when  
361 monsoonal rainfall during summer seasons weakened.

362 In northwestern Madagascar, stalagmite deposition during the MEHI and the MLHI could  
363 suggest sufficient dripwater supply that could reflect wetter conditions, linked to southward mean  
364 position of the ITCZ. The hiatus in deposition during the MMHI could suggest a northward  
365 migration of the ITCZ. Factors that could influence the mean position of the ITCZ include change  
366 in insolation, difference in temperature between the two hemispheres, glaciers advances that  
367 indicate global cold conditions, and the alteration of the thermohaline circulation. These factors  
368 are discussed in detail further below.

369

### 370 **5.3.1. ITCZ and insolation**

371 The ITCZ migrates southward in austral summer and northward in boreal summer in  
372 response to seasonal insolation. This migration has also been observed at decadal, centennial, and  
373 millennial scale (e.g. Haug et al., 2001; Voarintsoa et al., 2016). If we assume that insolation is the  
374 sole driver of the ITCZ's latitudinal migration, comparison of the insolation curves of Berger and  
375 Loutre (1991) and the stable isotope profiles and the timing of deposition of stalagmites ANJB-2



376 and MAJ-5 (Fig. 5a) suggests that high winter insolation in the southern hemisphere could have  
377 been responsible of the southward migration of the ITCZ during the early Holocene. This could  
378 have increased the number of summer months in northwestern Madagascar, without necessarily  
379 intensifying the monsoon strength. On the other hand, the southward migration of the ITCZ during  
380 the late Holocene could be linked to high summer insolation (Fig. 5). In such conditions, it could  
381 be possible that monsoonal rainfall in northwestern Madagascar intensified (see Supplementary  
382 Text 1 and Fig. S9).

383 Recognizing that application of the insolation curve of Berger and Loutre (1991) to  
384 paleohydrology in northwestern Madagascar might seem subjective, we also compared our  
385 records with the solar radiation reconstruction from  $^{14}\text{C}$  residual records of Stuiver et al. (1998).  
386 The stalagmite  $\delta^{18}\text{O}$  records relate well to the reconstructed solar irradiance fluctuations during  
387 the early Holocene. Negative  $\delta^{18}\text{O}$  values, indicative of wetter conditions in northwestern  
388 Madagascar, correspond to high  $\Delta^{14}\text{C}$  residuals values, indicative of low solar irradiance (Fig. 5). A  
389 similar but opposite relationship has been observed during the Holocene Asian Monsoon in  
390 Dongge Cave, southern China, a region visited by the ITCZ during boreal summers (Wang et al.,  
391 2005). Figure 2 of Wang et al. (2005) suggests that higher solar irradiance (smaller  $\Delta^{14}\text{C}$ )  
392 corresponds to a stronger Asian Monsoon. This antiphase relationship between northwestern  
393 Madagascar and southern China's monsoonal response, for example, could suggest that the  
394 distribution of energy related to solar irradiance leads to shifts of the ITCZ, and this is felt in both  
395 hemispheres.

396 Comparing the stalagmite  $\delta^{18}\text{O}$  records with the same  $^{14}\text{C}$  residual records of Stuiver et al.  
397 (1998), the late Holocene paleohydrology linkage to insolation is not as obvious as the early  
398 Holocene. This could be explained by the complexity of the climate drivers during the late  
399 Holocene. Studies report that the late Holocene climate has changed in response to several  
400 overlapping effects of the orbitally driven insolation, volcanic eruptions, changes in solar  
401 irradiance (e.g. Wanner et al., 2008), and changes in regional to global-scale variations in  
402 temperature (e.g. Neukom et al., 2014; Chambers, 2015).

403 For the mid-Holocene, our inference of a drier Madagascar paleoclimate seems to agree  
404 with the paleoclimate simulation of Braconnot et al. (2007), suggesting that the northern



405 hemisphere insolation increased. This insolation hypothesis was briefly reviewed in Chiang (2009;  
406 see his Fig. 6). Per Chiang's review, the predominant climate forcing of the mid-Holocene  
407 (centered at ~6 ka) was a pronounced change to the insolation, which was primarily due to  
408 precessional changes in Earth's orbit. He added that the Earth was nearer to the Sun in boreal  
409 summer than boreal winter, and NH summers were more intense than today. Quantification of  
410 the mean ITCZ position using a set of coupled ocean-atmosphere(-vegetation) simulations during  
411 the Mid- Holocene (ca. ~6 ka) in the second phase of the Paleoclimate Modeling Intercomparison  
412 Project (PMIP2) suggests a northward displacement of the ITCZ at ~6 ka (Braconnot et al., 2007)  
413 in response to increased summer insolation (Braconnot et al., 2000). This northward migration  
414 increased the mean simulated precipitation over the northern edge of the ITCZ (Braconnot et al.,  
415 2007), but could have decreased the mean precipitation simulated over its southern edge, as in  
416 northwestern Madagascar (this study).

417

### 418 **5.3.2. Linkages to ocean-atmosphere dynamics: ITCZ and global cooling/warming conditions**

419 Besides insolation, the ITCZ's length of visit in either hemisphere also depends on global  
420 cooling/warming conditions (e.g. Chiang and Bitz, 2005; Broccoli et al., 2006). Global cooling  
421 and/or warming conditions are often reflected by the extent of glacial advances (e.g. Fig. 3 of  
422 Wanner et al., 2011). Model simulations using an AGCM– slab ocean model (Chiang and Bitz, 2005)  
423 suggest a southward shift in the ITCZ over all tropical ocean basins when extratropical cooling and  
424 enhanced sea-ice cover in the NH were imposed. Similar simulations revealed a northward shift in  
425 the ITCZ when a southern extratropical cooling was imposed, enhancing cooling in the SH (Broccoli  
426 et al., 2006). It has therefore been reported and widely agreed that the ITCZ's latitudinal migration  
427 is driven by the temperature gradient between the two hemispheres (Chiang and Bitz, 2005;  
428 Broccoli et al., 2006; Chiang and Friedman, 2012). The ITCZ moves from a cold hemisphere towards  
429 a warmer one (e.g. Kang et al., 2008; McGee et al., 2014; Talento and Barreiro, 2016), and this  
430 latitudinal migration has been the main driver of rainfall availability in tropical and semi-arid  
431 regions visited by the ITCZ at decadal to millennial scales (e.g. Haug et al., 2001; Voarintsoa et al.,  
432 2016).



433 Figure 6a suggests that deposition of Stalagmite ANJB-2 and MAJ-5 during the MEHI and the  
434 MLHI, i.e. the wetter interval, coincided with the timing of a southward migration of the ITCZ,  
435 when the NH was cooler than the SH (Marcott et al., 2013). This timing of southward migration of  
436 the ITCZ coincided with intervals of global cooler conditions with high number of glacial advances  
437 (Figs. 6b–c; Wanner et al., 2011). This scenario agrees well with the model of Chiang and Bitz  
438 (2005), and the climatic responses are very similar to what has been observed in northeastern  
439 Namibia (e.g. Voarintsoa et al., 2016). In contrast, the hiatus in deposition during the mid-  
440 Holocene, marking the Malagasy mid-Holocene dry period, was coeval with a warmer NH and  
441 cooler SH, suggesting a northward migration of the ITCZ. This scenario agrees with the model  
442 simulation of Broccoli et al. (2006).

443

#### 444 5.3.3. ITCZ and AMOC: southward migration of the ITCZ during the 8.2 ka event

445 Understanding the Atlantic Meridional Overturning Circulation (AMOC)'s influence on  
446 Madagascar's hydroclimate could complete gaps in understanding the global circulation,  
447 particularly in the SH. The AMOC, a component of the Thermohaline Circulation (THC) or the  
448 Global Ocean Conveyor (Stommel, 1958; Gordon, 1986; Broecker, 1992, 1992; Delworth et al.,  
449 2008), is an important component of the Earth's climate system (Broecker 1991, 1992; Weaver et  
450 al. 1999; Delworth et al., 2008). It plays an essential role in maintaining global climate by  
451 transporting a large amount of heat from northern high latitude regions, starting for example at  
452 the North Atlantic Deep Water (NADW), to several regions worldwide (e.g., Broecker 1992;  
453 Weaver et al. 1999). It connects localized high latitude sinking cold water in north Atlantic with  
454 tropical climate changes (e.g., Dong and Sutton 2002; Zhang and Delworth 2005). The AMOC was  
455 used to interpret the non-orbital periodicity (i.e. at millennial scale) of isotopic records, identified  
456 in ice cores, as a result of an abrupt influx of meltwater from the Laurentide ice sheet into the N.  
457 Atlantic Ocean (e.g. Alley et al., 1997; Barber et al., 1999).

458 A more fundamental impact of the changes in the AMOC is the alteration of the  
459 temperature gradient between the two hemispheres, known to have been responsible of the  
460 latitudinal shift of the ITCZ in the tropical Atlantic (e.g. Dong and Sutton, 2007; Delworth et al.,  
461 2008, p. 309). The 8.2 ka event, a significant short-lived cooling of the early Holocene (Alley et al.,





462 1997), revealed in northwestern Madagascar records as a wet interval (Figs. 3 and 7), is an ideal  
463 timeframe to investigate such “ocean-land-atmosphere” relationship during the early Holocene.  
464 The 8.2 ka event is a known interval of abrupt freshwater influx from the melting Laurentide ice  
465 sheet into the North Atlantic (Alley et al., 1997; Barber et al., 1999; Kleiven et al., 2008; Carlson et  
466 al., 2008; Renssen et al, 2010; Wiersma et al., 2011; Wanner et al., 2015). It is equivalent to the  
467 sharp peak of the Bond cycle number 5 (Bond et al. 1997, 2001). This influx of meltwater altered  
468 the density and salinity of the NADW. Thornalley et al. (2009) reported a decrease in the NADW  
469 salinity to approximately 34 p.s.u. during the early Holocene. This perturbation of the North  
470 Atlantic could partially or completely weaken the AMOC (e.g., Vellinga and Wood 2002; Dong and  
471 Sutton 2002, 2007; Dahl et al. 2005; Zhang and Delworth 2005). Weakening of the AMOC would  
472 result in a deepening of the thermocline level (Timmermann et al, 2005), which could eventually  
473 lead to an anomalous warming of the southern oceans.

474 In parallel to this, the weakening of the AMOC would result in a positive cooling feedback  
475 to NH regions because the Gulf Stream was shut down. This weakening of the AMOC would  
476 therefore cause a significant temperature gradient between the two hemispheres, with a cooler  
477 NH and warmer SH, suggesting a southward migration of the ITCZ during the 8.2 ka event. Thus,  
478 northwestern Madagascar become wet, as suggested by the more negative stalagmite  $\delta^{18}\text{O}$  and  
479  $\delta^{13}\text{C}$  values around the 8.2 ka event. This wetting could correspond to a stronger Malagasy  
480 monsoon during austral summers, a phenomenon identical to the South American Summer  
481 Monsoon, identified in Brazil (e.g. Cheng et al., 2009). In contrast, regions in the northern  
482 Hemisphere monsoon regions became dry as the Asian Monsoon and the East Asian Monsoon  
483 became weaker (e.g. Wang et al., 2005; Dykoski et al., 2005; Cheng et al., 2009; Liu et al., 2013).  
484

## 485 6. Conclusion

486 Petrography, mineralogy, and stable isotope records from Stalagmite ANJB-2, from Anjohibe  
487 Cave, and Stalagmite MAJ-5, from Anjokipoty Cave, all combine to suggest three distinct intervals  
488 of climatic change in Madagascar during the Holocene: a wet Malagasy early Holocene interval, a  
489 dry Malagasy mid Holocene interval, and a wet Malagasy late Holocene interval. The timing of  
490 stalagmite deposition during the Malagasy early and late-Holocene in northwestern Madagascar



491 could be attributed to a more southward migration and/or an expanded ITCZ, increasing the  
492 duration of the summer rainy seasons and/or strengthening the intensity of the Malagasy  
493 monsoon. This could have been tied to insolation, the temperature gradient between the two  
494 hemispheres, and weakening of the AMOC. In contrast, the hiatus of deposition during the mid-  
495 Holocene, here named the Malagasy mid-Holocene dry period, could reflect a northward  
496 migration of the ITCZ, leading to drier conditions in northwestern Madagascar. The evidence of  
497 the 8.2 ka event in the Malagasy records further suggests a strong link between  
498 paleoenvironmental changes in Madagascar and abrupt climatic events in the Northern  
499 Hemisphere records, suggesting that Madagascar climate was also very sensitive to such abrupt  
500 climate events.

501

#### 502 **Author Contribution**

503 N.R.G.V. conceived the research and experiments. N.R.G.V, G.K, A.F.M.R, and M.O.M.R did the  
504 fieldwork and collected the samples. X.L., G.K., H.C., R.L.E, and N.R.G.V contributed to the <sup>230</sup>Th  
505 dating analyses. N.R.G.V provided detailed investigation of the two stalagmites, provided stable  
506 isotope measurements, prepared thin sections, and conducted X-ray diffraction analyses. G.K. also  
507 assisted with the isotopic measurements on Stalagmite ANJB-2. N.R.G.V. wrote the first draft of  
508 the manuscript and led the writing. L.B.R. provided a thorough review of the draft. N.R.G.V. and  
509 L.B.R. discussed and revised the manuscript, with additional comments from G.A.B and L.W.  
510 N.R.G.V revised the paper with input from all authors.

511

#### 512 **Competing Interests**

513 The authors declare no conflict of interest.

#### 514 **Acknowledgments**

515 This work was supported by grants from (1) the National Natural Science Foundation of China  
516 (NSFC 41230524, NBRP 2013CB955902, and NSFC 41472140) to Hai Cheng and Gayatri Kathayat,  
517 (2) the Geological Society of America Research Grant (GSA 11166-16) and John Montagne Fund  
518 Award, (3) the Miriam Watts-Wheeler Graduate Student Grant from the Department of Geology  
519 at UGA, and (4) the International Association of Sedimentology Post-Graduate Grant to N.



520 Voarintsoa. We also thank the Schlumberger Foundation for providing additional support to N.  
521 Voarintsoa's research. We thank the Department of Geology at the University of Antananarivo, in  
522 Madagascar, the Ministry of Energy and Mines, the local village and guides in Majunga for easing  
523 our research in Madagascar. We thank Pr. Paul Schroeder for giving us access to use the X-ray  
524 diffractometer of the Geology Department to conduct analysis on the mineralogy of the two  
525 stalagmites. We also thank Pr. Sally Walker for allowing us to use the microscope of the  
526 paleontology lab and for helping us photograph the stalagmites at very high resolution. We also  
527 thank Prof. John Chiang of the University of California in Berkeley, for sharing his thoughts and  
528 guiding us to useful literatures that are relevant to this work.  
529



530        **References**

- 531        Alley, R. B., Mayewski, P. A., Sowers, T., Stuiver, M., Taylor, K. C., and Clark, P. U.: Holocene climatic  
532                instability: A prominent, widespread event 8200 yr ago, *Geology*, 25, 483-486, 1997.
- 533        Barber, D. C., Dyke, A., Hillaire-Marcel, C., Jennings, A. E., Andrews, J. T., Kerwin, M. W., Bilodeau,  
534                G., McNeely, R., Southon, J., Morehead, M. D., and Gagnon, J. M.: Forcing of the cold event  
535                of 8,200 years ago by catastrophic drainage of Laurentide lakes, *Nature*, 400, 344-348, Doi  
536                10.1038/22504, 1999.
- 537        Berger, A., and Loutre, M. F.: Insolation Values for the Climate of the Last 10 million years,  
538                *Quaternary Sci Rev*, 10, 297-317, Doi 10.1016/0277-3791(91)90033-Q, 1991.
- 539        Bond, G., Kromer, B., Beer, J., Muscheler, R., Evans, M. N., Showers, W., Hoffmann, S., Lotti-Bond,  
540                R., Hajdas, I., and Bonani, G.: Persistent solar influence on north Atlantic climate during the  
541                Holocene, *Science*, 294, 2130-2136, Doi 10.1126/Science.1065680, 2001.
- 542        Bond, G., Showers, W., Cheseby, M., Lotti, R., Almasi, P., deMenocal, P., Priore, P., Cullen, H.,  
543                Hajdas, I., and Bonani, G.: A pervasive millennial-scale cycle in North Atlantic Holocene and  
544                glacial climates, *Science*, 278, 1257-1266, DOI 10.1126/science.278.5341.1257, 1997.
- 545        Braconnot, P., Marti, O., Joussaume, S., and Leclainche, Y.: Ocean feedback in response to 6 kyr BP  
546                insolation, *J Climate*, 13, 1537-1553, 2000.
- 547        Braconnot, P., Otto-Bliesner, B., Harrison, S., Joussaume, S., Peterchmitt, J. Y., Abe-Ouchi, A.,  
548                Crucifix, M., Driesschaert, E., Fichfet, T., Hewitt, C. D., Kageyama, M., Kitoh, A., Laine, A.,  
549                Loutre, M. F., Marti, O., Merkel, U., Ramstein, G., Valdes, P., Weber, S. L., Yu, Y., and Zhao,  
550                Y.: Results of PMIP2 coupled simulations of the Mid-Holocene and Last Glacial Maximum -  
551                Part 1: experiments and large-scale features, *Clim Past*, 3, 261-277, 2007.
- 552        Broccoli, A. J., Dahl, K. A., and Stouffer, R. J.: Response of the ITCZ to Northern Hemisphere cooling,  
553                *Geophys Res Lett*, 33, 10.1029/2005gl024546, 2006.
- 554        Broecker, W. S.: The Great Ocean Conveyor, *Oceanography*, 4, 79-89, 1991.
- 555        Broecker, W. S.: The Great Ocean Conveyor, *Global Warming: Physics and Facts*, 247, 129-161,  
556                1992.



- 557 Brook, G. A., Rafter, M. A., Railsback, L. B., Sheen, S. W., and Lundberg, J.: A high-resolution proxy  
558 record of rainfall and ENSO since AD 1550 from layering in stalagmites from Anjohibe Cave,  
559 Madagascar, Holocene, 9, 695-705, Doi 10.1191/095968399677907790, 1999.
- 560 Burney, D. A., Burney, L. P., Godfrey, L. R., Jungers, W. L., Goodman, S. M., Wright, H. T., and Jull,  
561 A. J. T.: A chronology for late prehistoric Madagascar, Journal of Human Evolution, 47, 25-  
562 63, Doi 10.1016/J.jhevol.2004.05.005, 2004.
- 563 Burney, D. A., James, H. F., Grady, F. V., Rafamantanantsoa, J. G., Ramilisonina, Wright, H. T., and  
564 Cowart, J. B.: Environmental change, extinction and human activity: evidence from caves  
565 in NW Madagascar, Journal of Biogeography, 24, 755-767, 10.1046/J.1365-  
566 2699.1997.00146.X, 1997.
- 567 Burney, D. A.: Late Quaternary Stratigraphic Charcoal Records from Madagascar, Quaternary Res,  
568 28, 274-280, Doi 10.1016/0033-5894(87)90065-2, 1987a.
- 569 Burney, D. A.: Late Holocene Vegetational Change in Central Madagascar, Quaternary Res, 28, 130-  
570 143, Doi 10.1016/0033-5894(87)90038-X, 1987.
- 571 Burns, S. J., Godfrey, L. R., Faina, P., McGee, D., Hardt, B., Ranivoharimanana, L., and Randrianasy,  
572 J.: Rapid human-induced landscape transformation in Madagascar at the end of the first  
573 millennium of the Common Era, Quaternary Sci Rev, 134, 92-99,  
574 10.1016/j.quascirev.2016.01.007, 2016.
- 575 Cabrol, P., and Coudray, J.: Climatic fluctuations influence the genesis and diagenesis of carbonate  
576 speleothems in southwestern France, National Speleological Society Bulletin 44, 112-117,  
577 1982.
- 578 Carlson, A. E., Legrande, A. N., Oppo, D. W., Came, R. E., Schmidt, G. A., Anslow, F. S., Licciardi, J.  
579 M., and Obbink, E. A.: Rapid early Holocene deglaciation of the Laurentide ice sheet, Nat  
580 Geosci, 1, 620-624, 10.1038/ngeo285, 2008.
- 581 Chambers, F. M.: The 'Little Ice Age': The first virtual issue of the Holocene, The Holocene, Epub  
582 ahead of print 29 June, DOI: 10.1177/0959683615593688, 2015.
- 583 Cheng, H., Fleitmann, D., Edwards, R. L., Wang, X. F., Cruz, F. W., Auler, A. S., Mangini, A., Wang, Y.  
584 J., Kong, X. G., Burns, S. J., and Matter, A.: Timing and structure of the 8.2 kyr BP event



- 585           inferred from delta O-18 records of stalagmites from China, Oman, and Brazil, *Geology*, 37,  
586           1007-1010, 10.1130/G30126a.1, 2009.
- 587   Chiang, J. C. H.: The Tropics in Paleoclimate, *Annual Review of Earth and Planetary Sciences*, 37,  
588           263-297, 10.1146/annurev.earth.031208.100217, 2009.
- 589   Chiang, J. C. H., and Bitz, C. M.: Influence of high latitude ice cover on the marine Intertropical  
590           Convergence Zone, *Clim Dynam*, 25, 477-496, 10.1007/s00382-005-0040-5, 2005.
- 591   Chiang, J. C. H., and Friedman, A. R.: Extratropical Cooling, Interhemispheric Thermal Gradients,  
592           and Tropical Climate Change, *Annual Review of Earth and Planetary Sciences*, 40, 383-412,  
593           10.1146/Annurev-Earth-042711-105545, 2012.
- 594   Crowley, B. E.: A refined chronology of prehistoric Madagascar and the demise of the megafauna,  
595           *Quaternary Sci Rev*, 29, 2591-2603, Doi 10.1016/J.Quascirev.2010.06.030, 2010.
- 596   Crowley, B. E., and Samonds, K. E.: Stable carbon isotope values confirm a recent increase in  
597           grasslands in northwestern Madagascar, *The Holocene*, 23, 1066-1073, Doi  
598           10.1177/0959683613484675, 2013.
- 599   Crowther, A., Lucas, L., Helm, R., Horton, M., Shipton, C., Wright, H. T., Walshaw, S., Pawlowicz,  
600           M., Radimilahy, C., Douka, K., Picornell-Gelabert, L., Fuller, D. Q., and Boivin, N. L.: Ancient  
601           crops provide first archaeological signature of the westward Austronesian expansion, *P*  
602           *Natl Acad Sci USA*, 113, 6635-6640, 10.1073/pnas.1522714113, 2016.
- 603   Dahl, K., Broccoli, A., and Stouffer, R.: Assessing the role of North Atlantic freshwater forcing in  
604           millennial scale climate variability: a tropical Atlantic perspective, *Clim Dynam*, 24, 325-  
605           346, 10.1007/s00382-004-0499-5, 2005.
- 606   Delworth, T. L., Clark, P. U., Holland, M., Johns, W. E., Kuhlbrodt, T., Lynch-Stieglitz, J., Morrill, C.,  
607           Seager, R., Weaver, A. J., and Zhang, R.: The potential for abrupt change in the Atlantic  
608           Meridional Overturning Circulation, in: *Abrupt Climate Change. A report by the U.S.*  
609           *Climate Change Science Program and the Subcommittee on Global Change Research. U.S.*  
610           *Geological Survey Reston, VA*, 117–162, 2008.
- 611   Dong, B. W., and Sutton, R. T.: Adjustment of the coupled ocean-atmosphere system to a sudden  
612           change in the Thermohaline Circulation, *Geophys Res Lett*, 29, 2002.



- 613 Dong, B., and Sutton, R. T.: Enhancement of ENSO variability by a weakened Atlantic thermohaline  
614 circulation in a coupled GCM, *J Climate*, 20, 4920-4939, 10.1175/Jcli4284.1, 2007.
- 615 Dutton, A., Bard, E., Antonioli, F., Esat, T. M., Lambeck, K., and McCulloch, M. T.: Phasing and  
616 amplitude of sea-level and climate change during the penultimate interglacial, *Nat Geosci*,  
617 2, 355-359, 10.1038/Ngeo470, 2009.
- 618 Dykoski, C. A., Edwards, R. L., Cheng, H., Yuan, D. X., Cai, Y. J., Zhang, M. L., Lin, Y. S., Qing, J. M.,  
619 An, Z. S., and Revenaugh, J.: A high-resolution, absolute-dated Holocene and deglacial  
620 Asian monsoon record from Dongge Cave, China, *Earth Planet Sc Lett*, 233, 71-86,  
621 10.1016/j.epsl.2005.01.036, 2005.
- 622 Fairchild, I. J., and Baker, A.: *Speleothem Science: From Processes to Past Environments*, edited  
623 by: Bradley, R., Wiley-Blackwell, 2012.
- 624 Frisia, S., Borsato, A., Fairchild, I. J., McDermott, F., and Selmo, E. M.: Aragonite–calcite  
625 relationships in speleothems (Grotte de Clamouse, France): environment, fabrics, and  
626 carbonate geochemistry., *J Sediment Res*, 772, 687-699, 2002.
- 627 Gasse, F., and Van Campo, E.: A 40,000-yr pollen and diatom record from Lake Tritrivakely,  
628 Madagascar, in the southern tropics, *Quaternary Res*, 49, 299-311, Doi  
629 10.1006/Qres.1998.1967, 1998.
- 630 Gommery, D., Ramanivosoa, B., Faure, M., Guerin, C., Kerloc'h, P., Senegas, F., and  
631 Randrianantenaina, H.: Oldest evidence of human activities in Madagascar on subfossil  
632 hippopotamus bones from Anjohibe (Mahajanga Province), *Cr Palevol*, 10, 271-278,  
633 10.1016/j.crpv.2011.01.006, 2011.
- 634 Gordon, A. L.: Inter-Ocean Exchange of Thermocline Water, *J Geophys Res-Oceans*, 91, 5037-5046,  
635 DOI 10.1029/JC091iC04p05037, 1986.
- 636 Haug, G. H., Hughen, K. A., Sigman, D. M., Peterson, L. C., and Rohl, U.: Southward migration of  
637 the intertropical convergence zone through the Holocene, *Science*, 293, 1304-1308, Doi  
638 10.1126/Science.1059725, 2001.
- 639 Head, M. J., and Gibbard, P. L.: Formal subdivision of the Quaternary System/Period: Past, present,  
640 and future, *Quatern Int*, 383, 4-35, 10.1016/j.quaint.2015.06.039, 2015.



- 641 Holmgren, K., Karlen, W., and Shaw, P. A.: Paleoclimatic Significance of the Stable Isotopic  
642 Composition and Petrology of a Late Pleistocene Stalagmite from Botswana, Quaternary  
643 Res, 43, 320-328, DOI 10.1006/qres.1995.1038, 1995.
- 644 Jungers, W. L., Demes, B., and Godfrey, L. R.: How big were the "Giant" extinct lemurs of  
645 Madagascar?, in: Elwyn Simons: A search for origins, edited by: Fleagle, J. G., and Gilbert,  
646 C. G., Springer, New York, 343-360, 2008.
- 647 Kang, S. M., Held, I. M., Frierson, D. M. W., and Zhao, M.: The response of the ITCZ to extratropical  
648 thermal forcing: Idealized slab-ocean experiments with a GCM, J Climate, 21, 3521-3532,  
649 10.1175/2007jcli2146.1, 2008.
- 650 Kim, S. T., O'Neil, J. R., Hillaire-Marcel, C., and Mucci, A.: Oxygen isotope fractionation between  
651 synthetic aragonite and water: Influence of temperature and Mg<sup>2+</sup> concentration,  
652 Geochim Cosmochim Ac, 71, 4704-4715, 10.1016/J.Gca.2007.04.019, 2007.
- 653 Kleiven, H. F., Kissel, C., Laj, C., Ninnemann, U. S., Richter, T. O., and Cortijo, E.: Reduced North  
654 Atlantic Deep Water coeval with the glacial Lake Agassiz freshwater outburst, Science, 319,  
655 60-64, 10.1126/science.1148924, 2008.
- 656 Lambert, W. J., and Aharon, P.: Controls on dissolved inorganic carbon and delta C-13 in cave  
657 waters from DeSoto Caverns: Implications for speleothem delta C-13 assessments,  
658 Geochim Cosmochim Ac, 75, 753-768, 10.1016/j.gca.2010.11.006, 2011.
- 659 Liu, Y. H., Henderson, G. M., Hu, C. Y., Mason, A. J., Charnley, N., Johnson, K. R., and Xie, S. C.: Links  
660 between the East Asian monsoon and North Atlantic climate during the 8,200 year event,  
661 Nat Geosci, 6, 117-120, 10.1038/Ngeo1708, 2013.
- 662 Ljungqvist, F. C.: The Spatio-Temporal Pattern of the Mid-Holocene Thermal Maximum, Geografie-  
663 Prague, 116, 91-110, 2011.
- 664 MacPhee, R. D. E., and Burney, D. A.: Dating of Modified Femora of Extinct Dwarf Hippopotamus  
665 from Southern Madagascar - Implications for Constraining Human Colonization and  
666 Vertebrate Extinction Events, J Archaeol Sci, 18, 695-706, Doi 10.1016/0305-  
667 4403(91)90030-S, 1991.





- 668 Marcott, S. A., Shakun, J. D., Clark, P. U., and Mix, A. C.: A Reconstruction of Regional and Global  
669 Temperature for the Past 11,300 Years, *Science*, 339, 1198-1201,  
670 10.1126/science.1228026, 2013.
- 671 Matsumoto, K., and Burney, D. A.: Late Holocene environments at Lake Mitsinjo, northwestern  
672 Madagascar, *The Holocene*, 4, 16-24, 1994.
- 673 Mayewski, P. A., Rohling, E. E., Stager, J. C., Karlen, W., Maasch, K. A., Meeker, L. D., Meyerson, E.  
674 A., Gasse, F., van Kreveld, S., Holmgren, K., Lee-Thorp, J., Rosqvist, G., Rack, F.,  
675 Staubwasser, M., Schneider, R. R., and Steig, E. J.: Holocene climate variability, *Quaternary*  
676 *Res*, 62, 243-255, Doi 10.1016/J.Yqres.2004.07.001, 2004.
- 677 McGee, D., Donohoe, A., Marshall, J., and Ferreira, D.: Changes in ITCZ location and cross-  
678 equatorial heat transport at the Last Glacial Maximum, Heinrich Stadial 1, and the mid-  
679 Holocene, *Earth Planet Sc Lett*, 390, 69-79, 10.1016/J.Epsl.2013.12.043, 2014.
- 680 Middleton, J., and Middleton, V.: Karst and caves of Madagascar, *Cave and Karst Science*, 29, 13-  
681 20, 2002.
- 682 Murray, J. W.: The deposition of calcite and aragonite in caves., *J Geol*, 62, 481-492, 1954.
- 683 Global Maps: Land Surface Temperature Anomaly.:  
684 [http://earthobservatory.nasa.gov/GlobalMaps/view.php?d1=MOD\\_LSTAD\\_M&d2=TRMM](http://earthobservatory.nasa.gov/GlobalMaps/view.php?d1=MOD_LSTAD_M&d2=TRMM)  
685 [\\_3B43M](http://earthobservatory.nasa.gov/GlobalMaps/view.php?d1=MOD_LSTAD_M&d2=TRMM), access: August 26th, 2016.
- 686 Nassor, A., and Jury, M. R.: Intra-seasonal climate variability of Madagascar. Part 1: Mean summer  
687 conditions, *Meteorol Atmos Phys*, 65, 31-41, Doi 10.1007/Bf01030267, 1998.
- 688 Neukom, R., Gergis, J., Karoly, D. J., Wanner, H., Curran, M., Elbert, J., Gonzalez-Rouco, F., Linsley,  
689 B. K., Moy, A. D., Mundo, I., Raible, C. C., Steig, E. J., van Ommen, T., Vance, T., Villalba, R.,  
690 Zinke, J., and Frank, D.: Inter-hemispheric temperature variability over the past millennium,  
691 *Nat Clim Change*, 4, 362-367, 10.1038/Nclimate2174, 2014.
- 692 Ottino, P.: Le Moyen-Age de l'Océan Indien et le peuplement de Madagascar, *Ann. Pays l'Océan*  
693 *Ind.*, 1, 197-221, 1974.
- 694 Paul, D., and Skrzypek, G.: Assessment of carbonate-phosphoric acid analytical technique  
695 performed using GasBench II in continuous flow isotope ratio mass spectrometry, *Int J*  
696 *Mass Spectrom*, 262, 180-186, 10.1016/j.ijms.2006.11.006, 2007.



- 697 Pobeguïn, T.: Sur les concrétions calcaires observés dans la Grotte de Moulis (Ariège), Société  
698 Géologique de la France, *Compte Rendus*, 241, 1791-1793, 1965.
- 699 Railsback, L. B., Akers, P. D., Wang, L. X., Holdridge, G. A., and Voarintsoa, N. R.: Layer-bounding  
700 surfaces in stalagmites as keys to better paleoclimatological histories and chronologies,  
701 *International Journal of Speleology*, 42, 167-180, 10.5038/1827-806x.42.3.1, 2013.
- 702 Railsback, L. B., Brook, G. A., Ellwood, B. B., Liang, F., Cheng, H., and Edwards, R. L.: A record of wet  
703 glacial stages and dry interglacial stages over the last 560 kyr from a standing massive  
704 stalagmite in Carlsbad Cavern, New Mexico, USA, *Palaeogeography, Palaeoclimatology,*  
705 *Palaeoecology*, 438, 256-266, 10.1016/j.palaeo.2015.08.010, 2015.
- 706 Railsback, L. B., Brook, G. A., Chen, J., Kalin, R., and Fleisher, C. J.: Environmental Controls on the  
707 Petrology of a Late Holocene Speleothem from Botswana with annual layers of aragonite  
708 and calcite, *J Sediment Res A*, 64, 147-155, 1994.
- 709 Railsback, L. B., Xiao, H. L., Liang, F. Y., Akers, P. D., Brook, G. A., Dennis, W. M., Lanier, T. E., Tan,  
710 M., Cheng, H., and Edwards, R. L.: A stalagmite record of abrupt climate change and  
711 possible Westerlies-derived atmospheric precipitation during the Penultimate Glacial  
712 Maximum in northern China, *Palaeogeogr Palaeocl*, 393, 30-44, Doi  
713 10.1016/J.Palaeo.2013.10.013, 2014.
- 714 Renssen, H., Goosse, H., Crosta, X., and Roche, D. M.: Early Holocene Laurentide Ice Sheet  
715 deglaciation causes cooling in the high-latitude Southern Hemisphere through oceanic  
716 teleconnection, *Paleoceanography*, 25, PA3204, doi10.1029/2009pa001854, 2010.
- 717 Romanek, C. S., Grossman, E. L., and Morse, J. W.: Carbon Isotopic Fractionation in Synthetic  
718 Aragonite and Calcite - Effects of Temperature and Precipitation Rate, *Geochim*  
719 *Cosmochim Ac*, 56, 419-430, Doi 10.1016/0016-7037(92)90142-6, 1992.
- 720 Saint-Ours, J. D.: Les phénomènes karstiques à Madagascar, *Annales de Spéléologie*, 14, 275-291,  
721 1959.
- 722 Schneider, T., Bischoff, T., and Haug, G. H.: Migrations and dynamics of the intertropical  
723 convergence zone, *Nature*, 513, 45-53, 10.1038/Nature13636, 2014.
- 724 Scholz, D., and Hoffmann, D. L.: StalAge - An algorithm designed for construction of speleothem  
725 age models, *Quat Geochronol*, 6, 369-382, 10.1016/j.quageo.2011.02.002, 2011.



- 726 Scholz, D., Hoffmann, D. L., Hellstrom, J., and Ramsey, C. B.: A comparison of different methods  
727 for speleothem age modelling, *Quat Geochronol*, 14, 94-104,  
728 10.1016/j.quageo.2012.03.015, 2012.
- 729 Zisu, N. S., Schwarcz, H. P., Konyer, N., Chow, T., and Noseworthy, M. D.: Macroholes in stalagmites  
730 and the search for lost water, *J Geophys Res-Earth*, 117, F03020, Doi  
731 10.1029/2011jf002288, 2012.
- 732 Siegel, F. R.: Aspects of calcium carbonate deposition in Great Onyx Cave, Kentucky,  
733 *Sedimentology*, 4, 285–299, 1965.
- 734 Siegel, F. R.: Calcite aragonite speleothems from a hand dug cave in northeast Kansas,  
735 *International Journal of Speleology* 2, 165-169, 1966.
- 736 Skrzypek, G., and Paul, D.: Delta C-13 analyses of calcium carbonate: comparison between the  
737 GasBench and elemental analyzer techniques, *Rapid Commun Mass Sp*, 20, 2915-2920,  
738 10.1002/rcm.2688, 2006.
- 739 Sletten, H. R., Railsback, L. B., Liang, F. Y., Brook, G. A., Marais, E., Hardt, B. F., Cheng, H., and  
740 Edwards, R. L.: A petrographic and geochemical record of climate change over the last 4600  
741 years from a northern Namibia stalagmite, with evidence of abruptly wetter climate at the  
742 beginning of southern Africa's Iron Age, *Palaeogeogr Palaeocl*, 376, 149-162, Doi  
743 10.1016/J.Palaeo.2013.02.030, 2013.
- 744 Stommel, H.: The Abyssal Circulation, *Deep-Sea Res*, 5, 80-82, Doi 10.1016/S0146-6291(58)80014-  
745 4, 1958.
- 746 Stuiver, M., Reimer, P. J., Bard, E., Beck, J. W., Burr, G. S., Hughen, K. A., Kromer, B., McCormac,  
747 G., Van der Plicht, J., and Spurk, M.: INTCAL98 radiocarbon age calibration, 24,000-0 cal  
748 BP, *Radiocarbon*, 40, 1041-1083, 1998.
- 749 Talento, S., and Barreiro, M.: Simulated sensitivity of the tropical climate to extratropical thermal  
750 forcing: tropical SSTs and African land surface, *Clim Dynam*, 47, 1091-1110,  
751 10.1007/s00382-015-2890-9, 2016.
- 752 Thornalley, D. J. R., Elderfield, H., and McCave, I. N.: Holocene oscillations in temperature and  
753 salinity of the surface subpolar North Atlantic, *Nature*, 457, 711-714,  
754 10.1038/nature07717, 2009.



- 755 Thrailkill, J.: Carbonate Deposition in Carlsbad Caverns, *J Geol*, 79, 683-695, 1971.
- 756 Timmermann, A., An, S. I., Krebs, U., and Goosse, H.: ENSO suppression due to weakening of the  
757 North Atlantic thermohaline circulation, *J Climate*, 18, 3122-3139, Doi  
758 10.1175/Jcli3495.1, 2005.
- 759 Vasey, N., Burney, D. A., and Godfrey, L.: Coprolites associated with *Archaeolemur* remains in  
760 North-western Madagascar suggest dietary diversity and cave use in a subfossil prosimian,  
761 in: *Leaping Ahead: Advances in Prosimian Biology*, edited by: Masters, J., Gamba, M., and  
762 Génin, F., Springer, New York, NY, 149–156, 2013.
- 763 Vellinga, M., and Wood, R. A.: Global climatic impacts of a collapse of the Atlantic thermohaline  
764 circulation, *Climatic Change*, 54, 251-267, Doi 10.1023/A:1016168827653, 2002.
- 765 Vinther, B. M., Buchardt, S. L., Clausen, H. B., Dahl-Jensen, D., Johnsen, S. J., Fisher, D. A., Koerner,  
766 R. M., Raynaud, D., Lipenkov, V., Andersen, K. K., Blunier, T., Rasmussen, S. O., Steffensen,  
767 J. P., and Svensson, A. M.: Holocene thinning of the Greenland ice sheet, *Nature*, 461, 385-  
768 388, 10.1038/nature08355, 2009.
- 769 Virah-Sawmy, M., Willis, K. J., and Gillson, L.: Evidence for drought and forest declines during the  
770 recent megafaunal extinctions in Madagascar, *Journal of Biogeography*, 37, 506-519, Doi  
771 10.1111/J.1365-2699.2009.02203.X, 2010.
- 772 Virah-Sawmy, M., Willis, K. J., and Gillson, L.: Threshold response of Madagascar's littoral forest to  
773 sea-level rise, *Global Ecol Biogeogr*, 18, 98-110, 10.1111/j.1466-8238.2008.00429.x, 2009.
- 774 Voarintsoa, N. R. G., Brook, G. A., Liang, F., Marais, E., Hardt, B., Cheng, H., Edwards, R. L., and  
775 Railsback, L. B.: Stalagmite multi-proxy evidence of wet and dry intervals in northeastern  
776 Namibia: linkage to latitudinal shifts of the Inter-Tropical Convergence Zone and changing  
777 solar activity from AD 1400 to 1950, *The Holocene*, In press, 1-13,  
778 doi:10.1177/0959683616660170, 2016.
- 779 Voarintsoa, N.R. G., Wang, L., Railsback, L.B., Brook, G.A., Liang, F., Cheng, H., Edwards, R.L.:  
780 Multiple proxy analyses of a U/Th-dated stalagmite to reconstruct paleoenvironmental  
781 changes in northwestern Madagascar between AD 370 and AD 1300, *Palaeogeography*,  
782 *Palaeoclimatology*, *Palaeoecology*, under review.



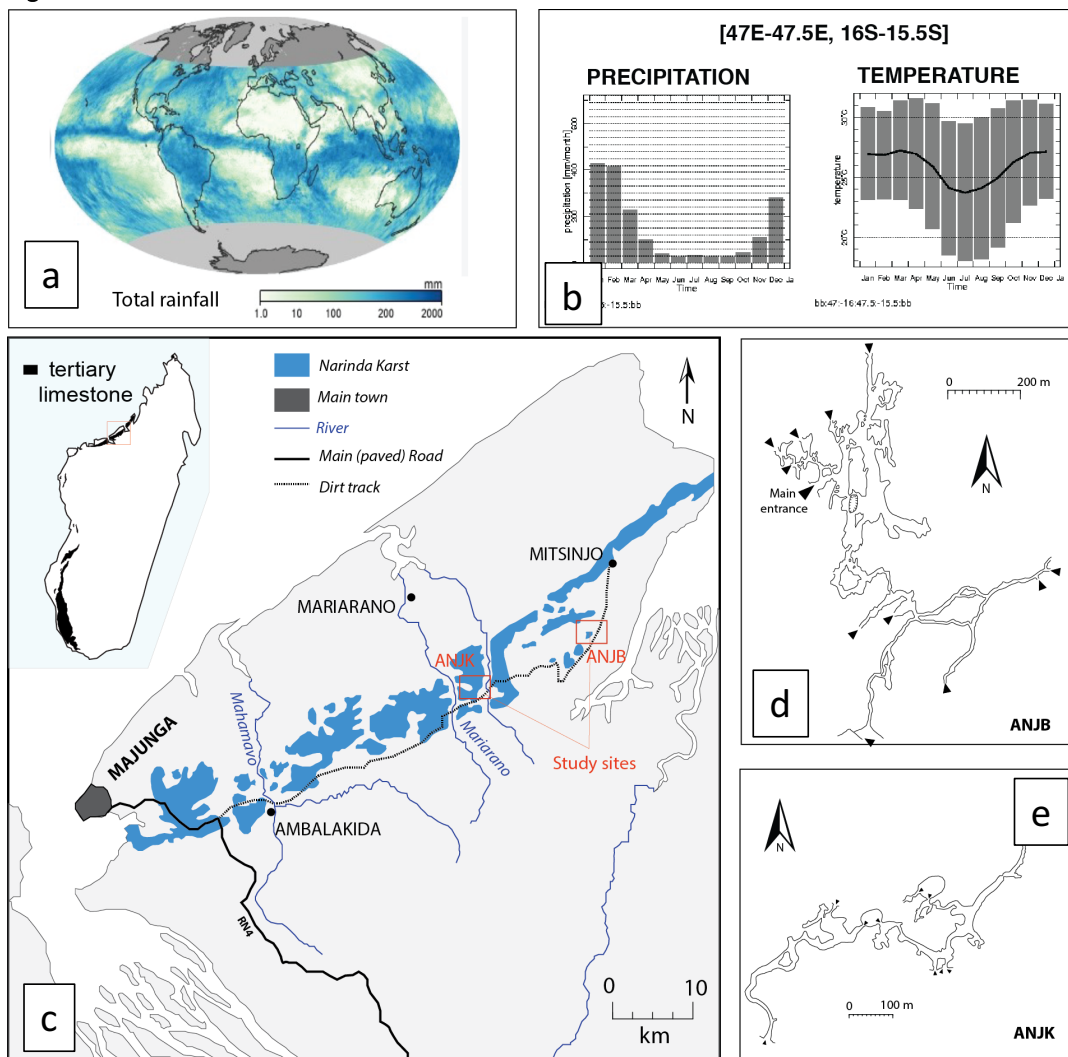
- 783 Walker, M. J. C., Berkelhammer, M., Bjorck, S., Cwynar, L. C., Fisher, D. A., Long, A. J., Lowe, J. J.,  
784 Newnham, R. M., Rasmussen, S. O., and Weiss, H.: Formal subdivision of the Holocene  
785 Series/Epoch: a Discussion Paper by a Working Group of INTIMATE (Integration of ice-core,  
786 marine and terrestrial records) and the Subcommission on Quaternary Stratigraphy  
787 (International Commission on Stratigraphy), *J Quaternary Sci*, 27, 649-659,  
788 10.1002/jqs.2565, 2012.
- 789 Wang, L., 2016. Late Quaternary paleoenvironmental changes in Southern Africa and Madagascar:  
790 evidence from aeolian, fluvial, and cave deposits. Unpublished dissertation. University of  
791 Georgia. 312p.
- 792 Wang, L. and Brook, G. A. 2013. Holocene climate changes in northwest Madagascar: evidence  
793 from a two-meter-long stalagmite from the Anjohibe Cave, Meeting Program of the  
794 Association of American Geographers, published online. Session 1512: Paleorecords of our  
795 Changing Earth I: Climate History and Human-Environment Interaction in the Old and New  
796 World Tropics, 2013.
- 797 Wang, Y. J., Cheng, H., Edwards, R. L., He, Y. Q., Kong, X. G., An, Z. S., Wu, J. Y., Kelly, M. J., Dykoski,  
798 C. A., and Li, X. D.: The Holocene Asian monsoon: Links to solar changes and North Atlantic  
799 climate, *Science*, 308, 854-857, 10.1126/science.1106296, 2005.
- 800 Wanner, H., and Ritz, S. P.: A web-based Holocene Climate Atlas (HOCLAT):  
801 [http://www.oeschger.unibe.ch/research/projects/holocene\\_atlas/](http://www.oeschger.unibe.ch/research/projects/holocene_atlas/), 2011.
- 802 Wanner, H., Beer, J., Butikofer, J., Crowley, T. J., Cubasch, U., Fluckiger, J., Goosse, H., Grosjean,  
803 M., Joos, F., Kaplan, J. O., Kuttel, M., Muller, S. A., Prentice, I. C., Solomina, O., Stocker, T.  
804 F., Tarasov, P., Wagner, M., and Widmann, M.: Mid- to Late Holocene climate change: an  
805 overview, *Quaternary Sci Rev*, 27, 1791-1828, 10.1016/j.quascirev.2008.06.013, 2008.
- 806 Wanner, H., Mercolli, L., Grosjean, M., and Ritz, S. P.: Holocene climate variability and change; a  
807 data-based review, *J Geol Soc London*, 172, 254-263, 10.1144/jgs2013-101, 2015.
- 808 Wanner, H., Solomina, O., Grosjean, M., Ritz, S. P., and Jetel, M.: Structure and origin of Holocene  
809 cold events, *Quaternary Sci Rev*, 30, 3109-3123, 10.1016/j.quascirev.2011.07.010, 2011.



810 Weaver, A. J., Bitz, C. M., Fanning, A. F., and Holland, M. M.: Thermohaline circulation: High-  
811 latitude phenomena and the difference between the Pacific and Atlantic, Annual Review  
812 of Earth and Planetary Sciences, 27, 231-285, DOI 10.1146/annurev.earth.27.1.231, 1999.  
813 Wiersma, A. P., Roche, D. M., and Renssen, H.: Fingerprinting the 8.2 ka event climate response in  
814 a coupled climate model, J Quaternary Sci, 26, 118-127, 10.1002/jqs.1439, 2011.  
815 Zhang, R., and Delworth, T. L.: Simulated tropical response to a substantial weakening of the  
816 Atlantic thermohaline circulation, J Climate, 18, 1853-1860, Doi 10.1175/Jcli3460.1, 2005.  
817



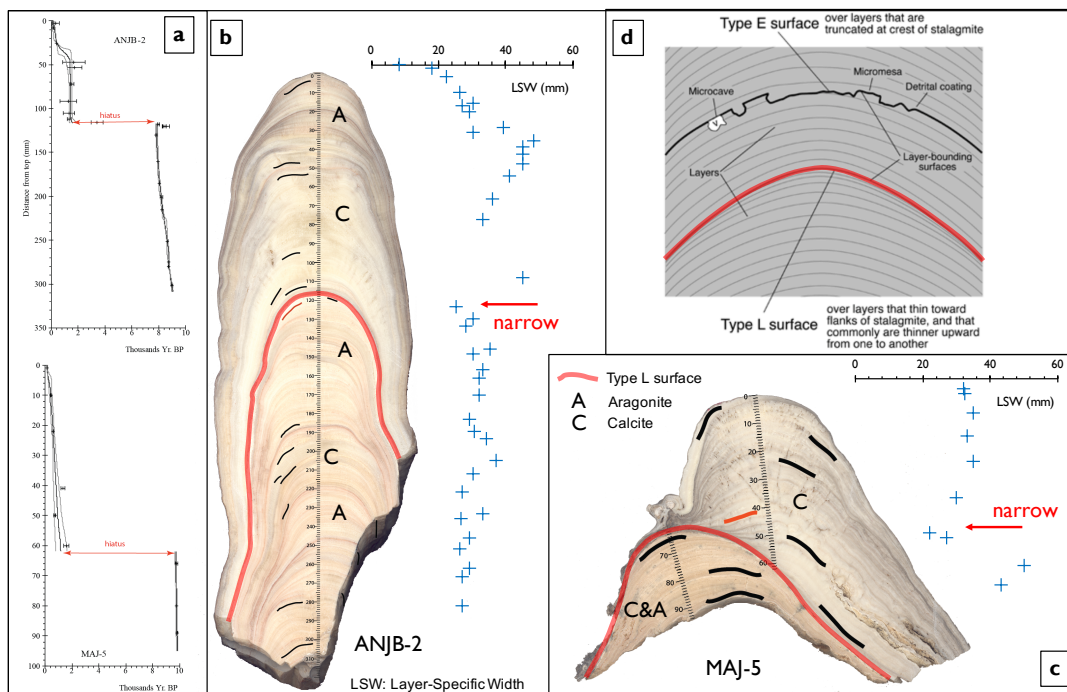
818 Figures



819  
 820 Figure 1: Climatological and geographic setting of Madagascar and the study area. (a) Global  
 821 rainfall maps recorded by NASA's Tropical Rainfall Measuring Mission (TRMM) satellite showing  
 822 the total monthly rainfall in millimeters and the overall position of the ITCZ during November,  
 823 2006. Darker blue shades indicate regions of higher rainfall (source: NASA Earth Observatory,  
 824 2016). (b) Barplots of the monthly climatology of precipitation, and the monthly average of daily  
 825 maximum, minimum, and mean temperature in northwestern Madagascar. The base period used  
 826 for the climatology is 1971-2000. Source: <http://iridl.ldeo.columbia.edu/> (accessed August 31,  
 827 2016). (c) Simplified map showing the southwest part of the Narinda karst and the location of the  
 828 study areas. Inset figure is a map of Madagascar showing the extent of the Tertiary limestone cover  
 829 that makes up the Narinda karst. (d-e) Maps of Anjohibe (ANJB) and Anjokipoty (ANJK) caves (St-

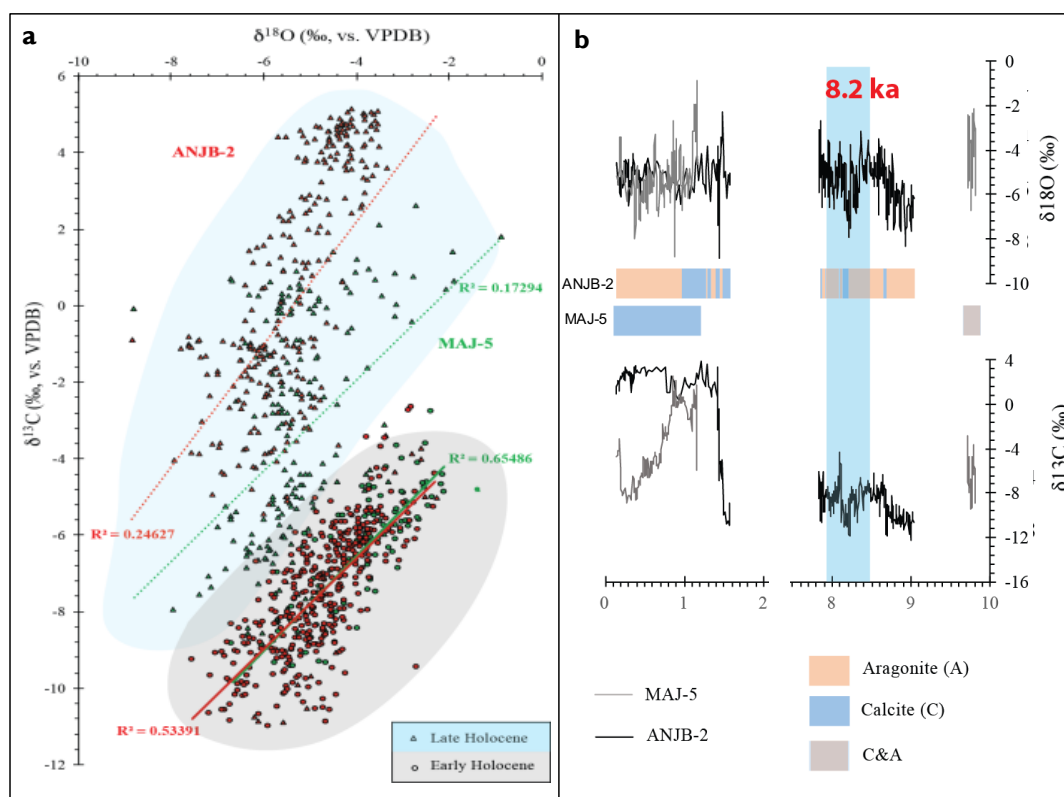


830 Ours, 1959; Middleton and Middleton, 2002). See Figs. S1–S3 for additional information about the  
831 study locations.  
832

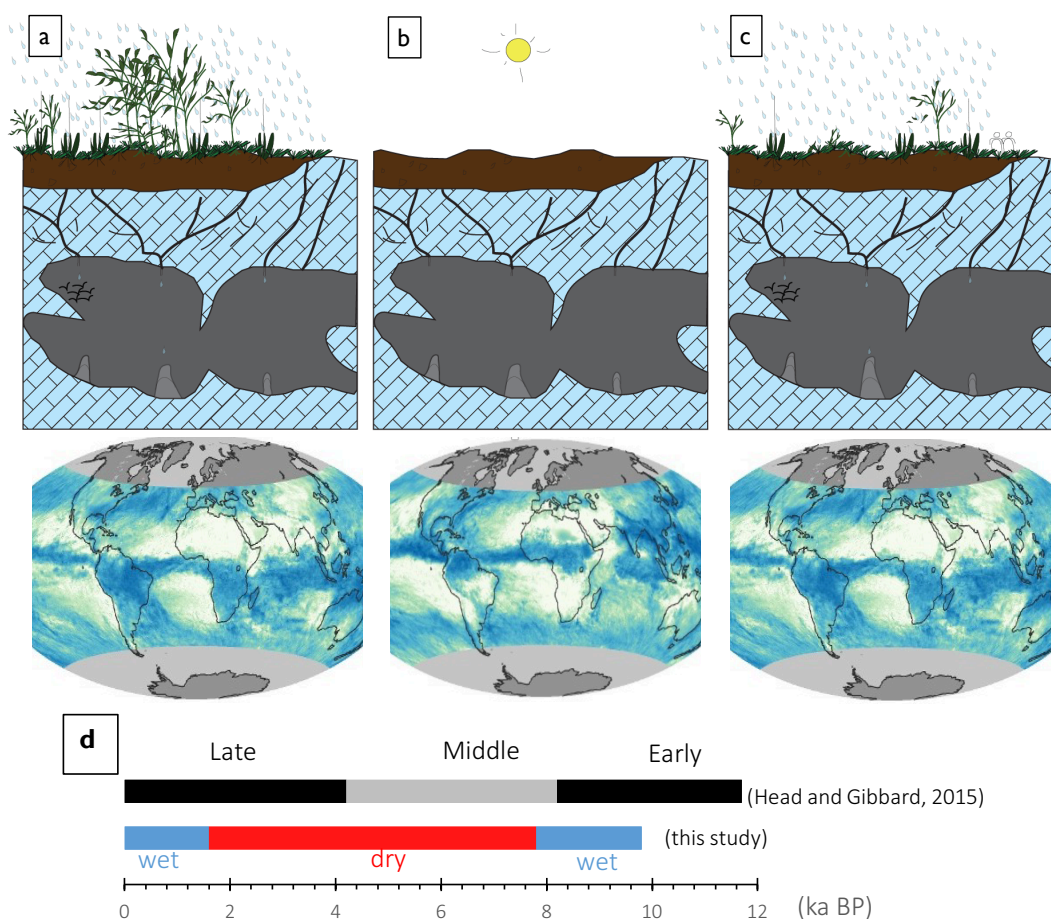


833  
834 Figure 2: Age model and petrography/mineralogy of Stalagmite ANJB-2 and MAJ-5. a) Age model  
835 constructed using the StalAge1.0 algorithm of Scholz and Hoffman (2011) and Scholz et al. (2012).  
836 b) Scanned image of Stalagmite ANJB-2 and the corresponding variations in layer-specific width  
837 (LSW). c) Scanned image of Stalagmite MAJ-5 and the corresponding layer-specific width (LSW). d)  
838 Sketches of typical layer-bounding surfaces (Type E and Type L) of Railsback et al. (2013). X-ray  
839 diffraction data are available in Fig. S5. Close-up of photographs of the hiatuses are shown in Fig  
840 S6.





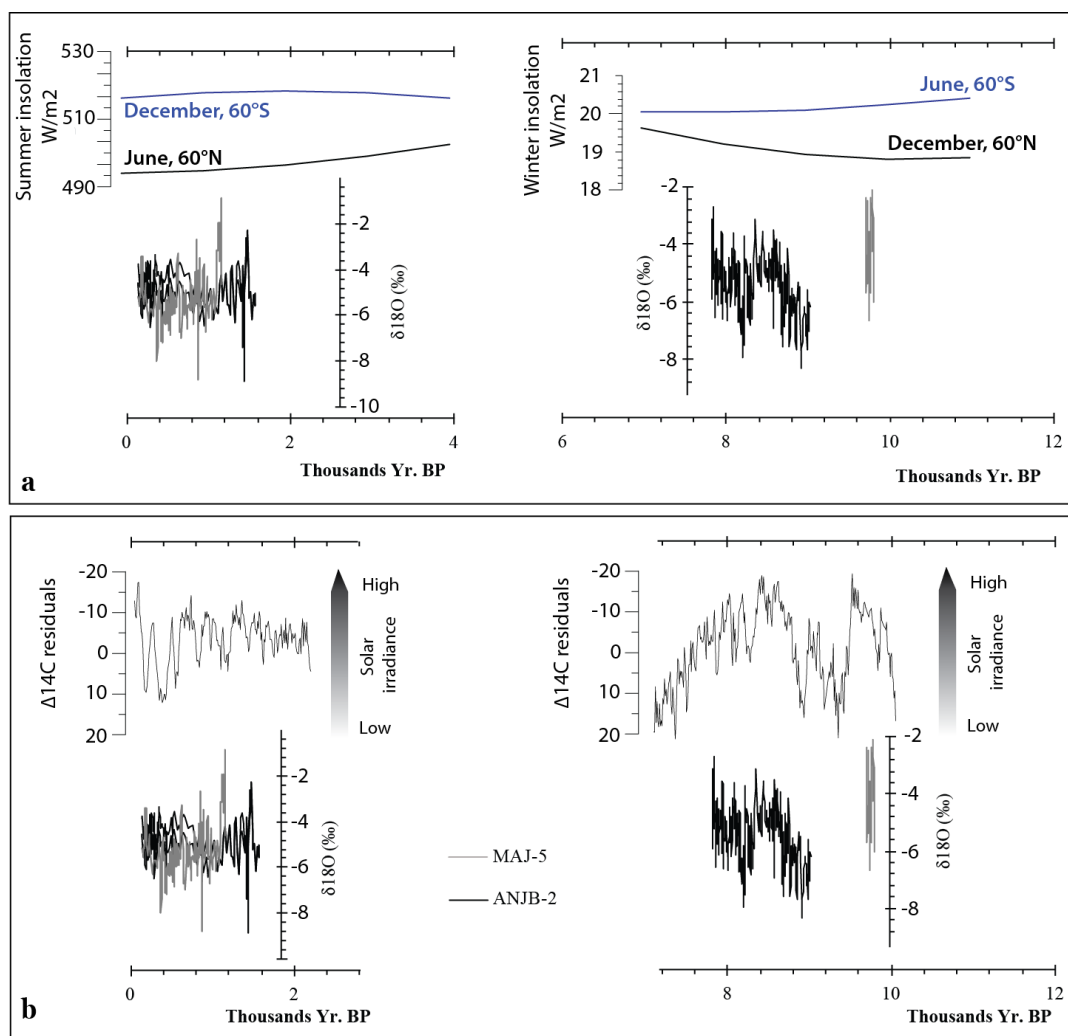
841  
842 Figure 3: **Stable isotope data.** a) Scatterplots of  $\delta^{13}\text{C}$  and  $\delta^{18}\text{O}$  for Stalagmite MAJ-5 (green) and  
843 ANJB-2 (red) during the Malagasy early Holocene interval (circle) and the Malagasy late Holocene  
844 interval (triangle). The plot shows distinctive early and late Holocene (roughly highlighted in gray  
845 and light blue shade, respectively). b) Stable isotope of oxygen and carbon profile of Stalagmite  
846 ANJB-2 and Stalagmite MAJ-5 with their corresponding mineralogy. More information about the  
847 late Holocene is presented in Fig. S7.  
848



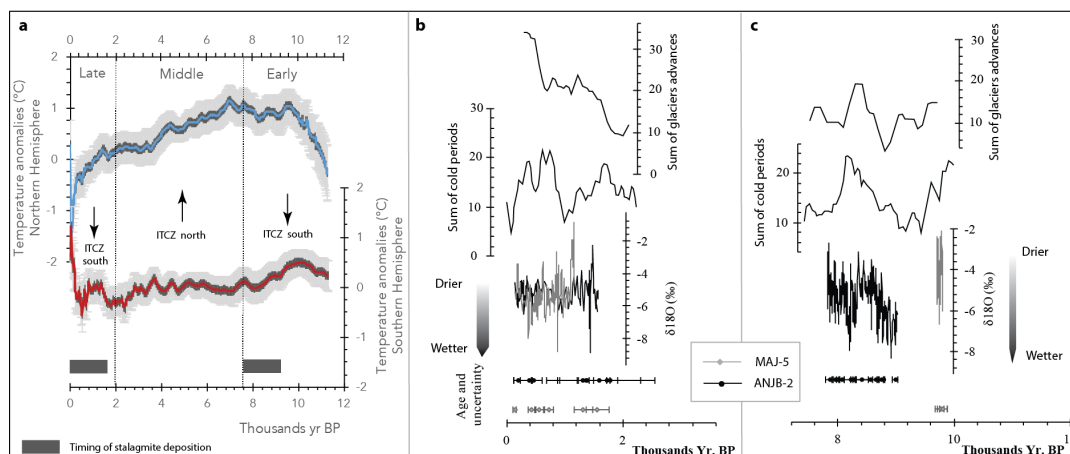
849

850

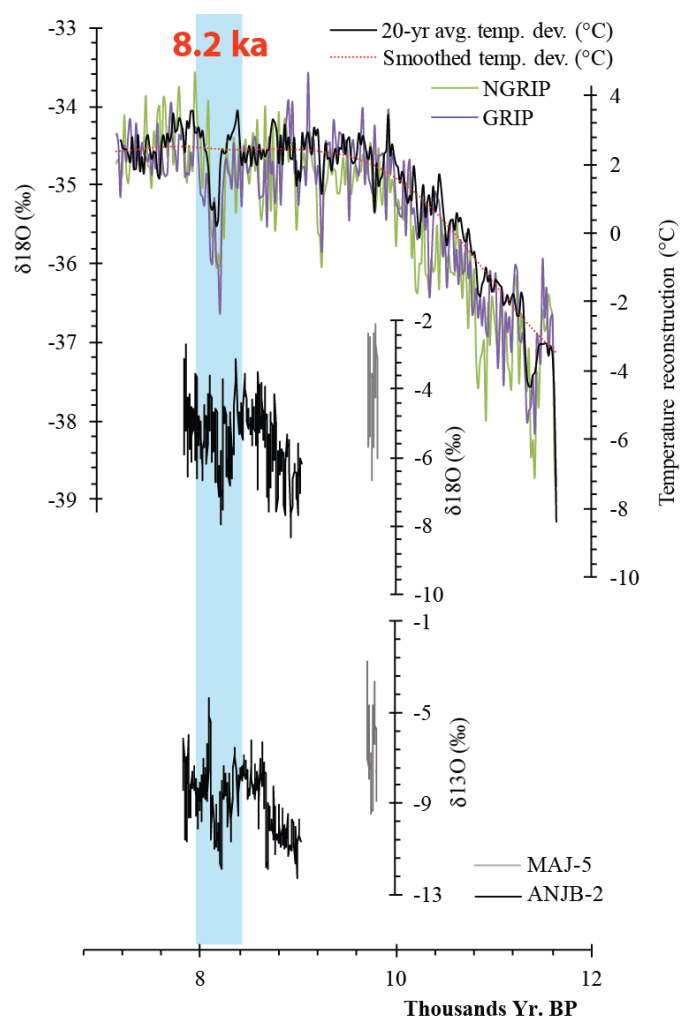
851 Figure 4: **Very simplified series of models portraying the Holocene climate change in northwestern**  
 852 **Madagascar and the possible climatic conditions linked to the ITCZ.** a) Wetter conditions during  
 853 the early Holocene with ITCZ south (prior to ca. 7.8 ka), favorable for stalagmite deposition. b)  
 854 Drier mid-Holocene with ITCZ north with no stalagmite formation. c) Wetter conditions during the  
 855 late Holocene (after ca. 1.6 ka) with ITCZ south, favorable for stalagmite deposition. For details  
 856 about paleo-vegetation reconstruction, refer to Sect. 5.2 and Fig. S7. Drawings are not to scale.  
 857 The bottom figures are from the same source as Fig. 1a, and they are only used here to give a  
 858 perspective of the possible position of the ITCZ during the early, mid, and late Holocene. d)  
 859 Comparison of the three Malagasy Holocene interval with the Head and Gibbard (2015)  
 860 subdivision (see text for details, Sect. 5.2).



861  
862 Figure 5: Paleoclimate of northwestern Madagascar compared with insolation. (a) Comparison  
863 between insolation curves (Berger and Loutre, 1991) and stalagmite  $\delta^{18}\text{O}$ . Timing of stalagmite  
864 deposition is coeval with high southern hemisphere winter insolation during the early Holocene  
865 and high southern hemisphere summer insolation during the late Holocene. (b) Reconstructed  
866 solar irradiance from  $\Delta^{14}\text{C}$  residuals (Stuiver et al., 1998) compared with Stalagmite  $\delta^{18}\text{O}$ .  
867 Stalagmite  $\delta^{18}\text{O}$  relates well to the reconstructed solar irradiance ( $\Delta^{14}\text{C}$ ), particularly during the  
868 early Holocene.



869  
870 Figure 6: Climate of NW Madagascar compared with global temperature conditions. a) Average  
871 Holocene temperatures in the Northern Hemisphere 90°–30°N (blue) and the Southern  
872 Hemisphere 90°–30°S (red), referenced to the 1961–1990 mean temperature (Marcott et al.,  
873 2013), with 1σ uncertainty (gray). b–c) Curves representing the sum of glaciers advances from a  
874 set of global Holocene time series compiled from natural paleoclimate archives (Wanner et al.,  
875 2011) and curves representing the sum of cold periods from a set of global Holocene time series  
876 compiled from natural paleoclimate archives (Wanner et al., 2011) compared with the δ<sup>18</sup>O profile  
877 of Stalagmite ANJB-2 (black) and MAJ-5 (gray) and their corresponding radiometric age data with  
878 the 2σ error.



879  
880 Figure 7: **The 8.2 ka event in Madagascar.** Oxygen isotope record from Greenland (GRIP and NGRIP)  
881 ice cores (Vinther et al., 2009) compared with Stalagmite ANJB-2  $\delta^{18}\text{O}$  and  $\delta^{13}\text{C}$ . Fig. S8 provides  
882 additional supporting evidence of the wet 8.2 ka event.